Reaction Chemistry & Engineering

ROYAL SOCIETY OF CHEMISTRY

PAPER

View Article Online
View Journal | View Issue

Cite this: *React. Chem. Eng.*, 2024, 9, 1776

Determination of intermediates and products of the uranyl aerosol formation in UF_6 hydrolysis in the gas phase†

Christian Mark Salvador,*[a] Jason M. Richards,[b] Shannon M. Mahurin,[c] Meng-Dawn Cheng*[a] and Joshua A. Hubbard[d]

The reaction pathway of hydrolysis of UF_6 to form UO_2F_2 particles is an essential insight in nuclear fuel processing; however, it is still limited to theoretical calculations. Herein, we present the identification of the intermediates and products using various gas precursor concentrations and molecular beam mass spectrometer (MBMS). Compounds containing different uranium atom counts were identified by exposing 300 and 2323 ppm water to 200 ppm UF_6. Non-uranium compounds (*e.g.*, $(HF)_3(H_2O)H$, $(HF)_4H$, and $(H_2O)_2(HF)_3$) dominate the mass spectra in terms of absolute signal intensity. These compounds were dependent on the initial concentration of UF_6 based on the linear relationship observed between products and gas reactant. Uranium compounds were characterized by UF_6, UO_3, and UO_2F_2 core molecules, with each species existing predominantly in a certain water concentration. Monomeric compounds (*e.g.*, $UF_6(HF)_2(H_2O)_7$, $UO_2F_2(HF)_7H$, and $UO_2F_2(HF)_5(H_2O)_3$) or species with one uranium atom had high fluorine to uranium ratio (F/U) due to several HF units bonded with the uranium core. Dimeric (*e.g.* $(UO_2F_2)_2(H_2O)$ and $(UF_6)_2(H_2O)4(HF)_3H$) and trimeric (*e.g.*, $(UO_3)(UO_2F_2)_2(HF)(H_2O)_3$ and $(UO_2F_2)_2UF_6H_2F$) compounds persisted in high masses with low F/U and H/U ratios. Moreover, ramping of UF_6 concentration (50–231 ppm) at fixed water content (1.3% Rh or 300 ppm) showed different trends among 949 ions, with some following consistently with molecular identification (*e.g.*, $(UO_3)_3(HF)_2(H_2O)H$). Overall, this study provided important information regarding the formation pathway of UO_2F_2, which will be essential in chemical modelling studies. The vast information generated from mass spectrometric runs merits cluster evaluation and factorization to yield more information on the U–O–F system.

Received 9th December 2023,
Accepted 4th March 2024

DOI: 10.1039/d3re00665d

rsc.li/reaction-engineering

1. Introduction

Uranyl fluoride (UO_2F_2) is an extremely stable product of UF_6, which is the chemical form of uranium used for enrichment procedures. UO_2F_2 plays a key role in the nuclear fuel production of UO_2 powder.[1,2] UF_6 instantaneously generates non-volatile UO_2F_2 and hydrogen fluoride (HF) upon contact with water.

The formation mechanism of the U–O–F system has been a subject of research since the 1960s. In the work of Otey and LeDoux,[3] they suggested the following hydrolysis reaction of UF_6:

$$UF_6(6) \underset{F_2}{\overset{H_2O}{\rightleftharpoons}} UOF_4(4) \underset{F_2}{\overset{H_2O}{\rightleftharpoons}} U_2O_3F_6(3) \underset{F_2}{\overset{H_2O}{\rightleftharpoons}} U_5O_3F_8(1.6) \underset{F_2}{\overset{H_2O}{\rightleftharpoons}} UO_2F_2(2) \underset{F_2}{\overset{H_2O}{\rightleftharpoons}} UO_3(0)$$

The values in the parenthesis are the fluorine to uranium (F/U) ratios, which sequentially decrease as the uranium compound is exposed to higher water content. Otey's and LeDoux's work also indicated that all the uranium species in the U–O–F system were successfully synthesized except for the UOF_4, which may be an indication of the low stability of such a compound. This has been the traditional research direction of UO_2F_2 formation. No recent experimental work has been implemented that probes the intermediates and products of UF_6 hydrolysis besides theoretical studies that provide information on the molecular systems of uranium species.

Previously, relativistic density functional theory calculations were used to model the hydrolysis of UF_6.[4] In that work, the reaction pathway was initiated by the 1:1 clustering of water and UF_6, which later forms UF_5OH upon the elimination of HF. Subsequent elimination of HF from

[a] *Environmental Sciences Division, Oak Ridge National Laboratory, Oak Ridge, TN, USA. E-mail: chengmd@ornl.gov*
[b] *Material Security and Counterproliferation Division, Oak Ridge, TN, USA*
[c] *Chemical Sciences Division, Oak Ridge National Laboratory, Oak Ridge, TN, USA*
[d] *Sandia National Laboratory, Albuquerque, NM, USA*

† Electronic supplementary information (ESI) available. See DOI: https://doi.org/10.1039/d3re00665d

the UF_5OH species yields UOF_4 compounds (*e.g.*, UOF_4, UOF_4·HF, and UOF_4·2HF), with some bonded with HF units. However, this process is endothermic (ΔE_a = 23.89 kcal mol^{-1}), which raises the question of whether the formation of such compounds and the overall reaction pathway are feasible without additional external energy. Integration of HF molecules into UOF_4 species can reduce the energy barrier but the initial reactions are still endothermic.[4] A complementary study from the same research group explored other reaction pathway conditions (*i.e.*, low temperature and or high UF_6 concentration) using the same theoretical approach.[5] This study proposed the dimeric species or compounds with two uranium atoms. The compounds include UF_6·UF_5OH, $(UF_5OH)_2$, $(UF_5)_2O$, and $U_2O_2F_9H$, which were assumed to initiate the solid formation. Interestingly, this reaction pathway is an exothermic reaction unlike the UOF_4 pathway discussed previously, which makes the reaction path more favourable at ambient conditions.

Recent experimental work probed the chemical kinetics and growth of the UO_2F_2 particles in water-lean conditions. Richards and colleagues[6] calculated a rate constant of 1.19 ± 0.22 $Torr^{-3/2}$ s^{-1} for the UF_6 hydrolysis using a Fourier transform infrared spectrometer with a 5 m long-path length gas cell. Analysis of the formation of UO_2F_2 particles using a series of mobility particle sizers and counters showed the dependence of this process on the concentration of water.[7] However, an in-depth examination of the participating intermediates and products of the UF_6 hydrolysis is required to further understand the gas-to-particle conversion of UF_6 to UO_2F_2. Here, species with varying uranium atom units, as well as HF and H_2O attached to the molecular core, were identified using a series of UF_6 hydrolysis with varying precursor concentrations. We report the experimental results by observing the intermediate species using a molecular beam mass spectrometer (MBMS) to detect intermediates and products with mass-to charge-ratio (m/z) between 50 to 1000 Dalton.

2. Experimental design

2.1. Reactant delivery and chamber manifold

A simplified manifold was designed that can deliver UF_6 and H_2O to the MBMS inlet, similar to a prior experimental setup.[7] The reactants were introduced in ultra-dry air (Parker, UDA-300) using an MKS mass flow controller (MFC) operated at 1 litre per minute (LPM). A concentrated UF_6 source U-tube provides sublimated gas. A subsequent U-tube in ice normalizes the flow of UF_6. The UF_6 gas is monitored online using a Fourier-transform infrared (FTIR) spectrometer (Bruker model ALPHA) at 1157 and 1290 cm^{-1} spectral bands. Water vapor is generated using a water bubbler and delivered to the chamber manifold at 1.0 LPM flow. Relative humidity (Rh) was modified using different combinations of flows of dry and wet air and monitored using a Vaisala hygrometer (model MI70). A steel manifold was constructed in front of the inlet of the MBMS. The manifold serves as the reaction platform where the UF_6 and H_2O are introduced and reacted with each other. Fig. 1 shows the schematic diagram of the manifold. Several two- and three-way valves were installed in the system to limit the flow of different reactant conditions that provide baseline and water requirements.

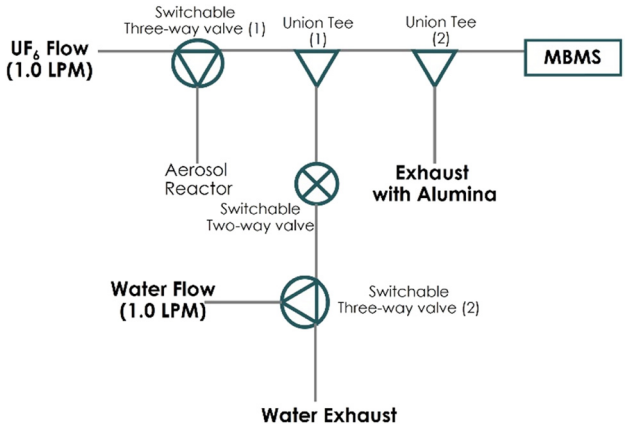

Fig. 1 Schematic diagram of the delivery manifold and the reaction chamber where the UF_6 hydrolysis occurs. The first switchable three-way valve directs the flow of UF_6 either to the reactor or the MBMS. The two-way switchable valve allows the conditioning of the lines with higher humidity, particularly from changing from dry to wet conditions. The alumina in the exhaust serves as the sink of the excess uranium and fluorinated compounds.

2.2. Mass spectra of UF_6 and limit of detection

The products of the UF_6 hydrolysis were monitored using an MBMS. Direct observation of highly reactive species formed during the reaction can be performed using the MBMS, in areas such as combustion, health, and atmospheric chemistry since the early 1990s.[15–17]

In our experimental setup (see Fig. 1), the UF_6 and H_2O met at the point labelled as the Union Tee (1), which we called the reaction point. The pressure at this point was approximately 1 atm and 20 °C. From this point on, the MBMS was about 15 cm long including the second Swagelok Tee (2), connection, and the inlet nozzle. A 100 μm orifice was used in the sampling train after the second Tee by the MBMS. With the low pressure inside Stage 1 of the MBMS being less than 1 torr, the gaseous mixture containing the residual reacting gases and cluster species as reaction products was drawn into Stage 1 by the pressure differential between the reacting point and Stage 1. The orifice creates a choked flow condition whereby 0.2 LPM of the 2 LPM was sampled into the MBMS and the remaining sample (that includes any residual reactants and products) was vented through the exhaust to an alumina treatment (see Fig. 1) before disposal.

The mixture sampled through the inlet nozzle of the MBMS expands right after the skimmer by design, which prevents additional collisions of the reacting atoms and molecules,[8] although the collisions in the throat of the nozzle are not discounted. Thus, additional modification on the

population of the clusters created by the hydrolysis was minimized by the beam expansion configuration. This sampling scheme has been used extensively in combustion research,[15–17] and the combination of MBMS and pyrolysis has also been widely used to determine the wood and lignin composition *in situ* and rapidly, which limits the unnecessary loss of the samples along the transfer lines.[9–11]

The VeraSpec MBx (Extrel, LLC) has an integrated cross-beam deflector ionizer design which provides a cleaner spectrum by separating the analyte ions from photon, metastable, particulates, and molecular beam gases. Stage 1 chamber in the MBMS system was typically operated between 0.4 to 0.7 torr. The pressure differential between the Stage 1 chamber (<1 torr) and the sampling inlet nozzle (~760 torr) was necessary to create a supersonic jet facilitating the delivery of the reaction products to the Stage 1. The potential for forming UF_6 neutral cluster species was highly unlikely as the average signal was only 15 for $(UF_6)_2$, mass = 704, at 200 ppm of UF_6 concentration, for example. The collision probability would be smaller for forming neutral UF_6 clusters of higher masses. The averaged UF_6 dimer signal (=15) was weaker than the averaged signal for neutral UF_6 (=86), mass 352. Furthermore, these signals were much weaker than the one shown in Fig. 2 for UF_5^+ mass 333 (~6500) used in the calibration curve.

Detailed analysis for the possible neutral cluster formation is discussed in the ESI† as supplemental material. Mass spectrometer data for the neutral clusters of $(UF_6)_n$ and $(H_2O)_n$, where n = 1 and 2 for the former species and 3 to 55 for the latter, were analysed and no detectable signals for the observable clusters of these two species were found. Whether the cluster species we reported were produced at the location before the mass spectrometer expansion beam or elsewhere in the mass spectrometer was analysed and reported in the ESI† as well.

We did not have direct experimental data to show that the cluster species were all produced before the sample entered the mass spectrometer due to (1) the complexity of refabricating parts for the experiment, (2) this topic was out of the scope of our study, and (3) our extensive experience with UF_6 chemistry and hydrolysis reaction in our aerosol reactor[7] (and references in the ESI†) suggested that the residual reactants left over from the reaction at the first Tee should be minimal if not zero. Nevertheless, we used computer simulations to provide indirect evidence showing that the signals detected by the MBMS were indeed cluster species produced through the reactions before they were sampled into the mass spectrometer as detailed in the ESI.†

Mass spectral data from m/z 50 to 1000 were acquired using electron ionization and a 4000 m/z quad mass filter. The mass calibration was performed by exposing the MBMS to the vapor of perfluorotributylamine (PFTBA) with a molar mass of 671.096 g mol^{-1}. PFTBA has fragments at peaks 69, 100, 131, 219, 264, 414, and 502, which were all used for the mass calibration. The Merlin Automation Data System Software (v3.3.1) was utilized for post-calibration, data extraction, and analysis.

Standard calibration of UF_6 was performed by modifying the mass flow of UF_6 and zero air introduced to the MBMS. The most prominent peak of UF_6 was mass 333, which corresponds to the UF_5^+ ion. The concentration of UF_6 was ramped from zero to 200 ppm, as shown in Fig. 2. Also in the same figure is the calibration curve of the signal intensity with the concentration of UF_6, in which a strong linear relationship is based on the coefficient of determination. The slight downward deviation of the low UF_6 concentration data in the left panel was caused by the sensitivity of the MFC at the low flow rate. The calculated limit of detection (L.O.D. = blank + 3 × standard deviation) was approximately 4.0 ppm.

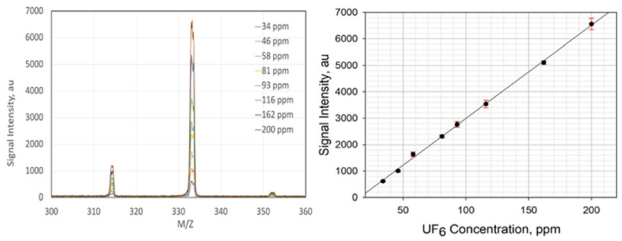

Fig. 2 (Left) Mass spectra of sequential increases of UF_6 concentration. (Right) Linear curve of the standard calibration of the UF_6 concentration and signal intensity of mass 333. The error bar is based on the standard deviation of each measurement.

2.3. Exposure of UF_6 to different water levels

Different concentration levels of UF_6 and H_2O were introduced to the manifold (see Fig. 1) and the MBMS to determine the reaction intermediates and products resulting from the UF_6 hydrolysis. Mass flow controller – metered UF_6 flow with constant 200 ppm concentration was exposed to water vapor concentration at 1.3% and 10% Rh performed with three trials on separate days. In separate experiments, constant water moisture was also introduced to the MBMS while ramping UF_6 from 0 to 231 ppm. Prior to the reaction of the UF_6 and water, the manifold and MBMS were exposed to UF_6 gas only to establish a baseline condition and enable the collection of a baseline spectrum. This step eliminates the possibility of interferences and artifacts contributing to the products obtained from the previous UF_6 hydrolysis experiment.

2.4. Peak identification

The mass spectra generated from different reaction conditions were scanned and peaks were picked based on their enhancement compared to the baseline condition (ultradry air only). Sixty mass spectra were collected at the end of measurements (~60 minutes), when equilibrium was assumed to be reached, and were averaged. Nominal peaks were only considered in the peak list if their percent increase was greater than 30%. Also, a peak should be present in all

three trials performed per experimental condition to be considered statistically significant.

Assignment of the molecular formula was implemented using ChemCalc, a web-based application programming interface.[12] ChemCalc provides suggested formulas based on a given atom range and accuracy. For this study, the following criteria for the number of atoms were constrained as follows: NU = 0–5, NH = 0–20, NF = 0–20, NO = 0–20, where NO = number of oxygen atoms contributing to the identified mass, NH = number of hydrogen atoms, NF = number of fluorine atoms, and NU = number of uranium atoms. We also assumed that all elements involved maintained their oxidation state over the course of the reaction [U(+6), F(−1), H(+1), and O(−2)]. U(6+) is a highly stable oxidation state for uranium molecules. That assumption excluded UO_2 and UF_5. The final reaction products containing uranium atom, *i.e.*, UO_2F_2, showed no evidence of change in the oxidation state so it is unlikely that a change in the oxidation state would occur in an intermediate species.

Peak locations of the ions were observed to drift approximately 0.6 Da, thus a ±1.0 nominal mass range error was considered sufficient for our system in choosing the appropriate molecular formula suggested by ChemCalc. The presence of other stable isotope variants such as oxygen 18 (O-18) was not considered due to the low concentration/signal of the peaks identified in the mass spectra. It is important to note that the ratio of relative abundance of O-18 to O-16 is close to 500 : 1. Thus, the probability of having oxygen isotope interference is quite low and also the sensitivity of our mass spectrometer is unable to detect such a low signal. The same goes for hydrogen, uranium, and fluorine atoms, in which the second most abundant isotopes do not interfere as much as to alter the mass identification and subsequent molecular formulation.

3. Results and discussion

3.1. Proposed molecular formula for identified species at variable water conditions

Table 1 lists the mass spectrum peaks that passed the criteria set in Sec 2.4. Peaks with a mass-to-charge ratio below 300 were tagged as non-uranium peaks. These compounds were identified as clusters of H_2O and HF. The most prominent peak among the non-uranium compounds is mass 81, which was assigned as the protonated cluster of four HF molecules, $(HF)_4H$. The source of this compound is assumed to be due to the polymerization of HF molecules, which is expected, given the high hydrogen bonding strength of HF.

Another formation pattern suggested is the direct emission of HF clusters from the hydrolysis of UF_6-H_2O, as shown in eqn (1).[13]

$$UF_6{\cdot}H_2O + H_2O \rightarrow UO_2F_2 + 4HF \quad (1)$$

Table 1 The proposed molecular formula of the UF_6 hydrolysis products. Included in the table is the water condition in which the peak showed higher concentration

Exp. mass	Proposed molecular formula	Theoretical isotopic mass	Dominant water condition (ppm)
79	$(HF)_3(H_2O)H$	79.037	Both
81	$(HF)_4H$	81.032	Both
96	$(H_2O)_2(HF)_3$	96.039	Both
155	$(H_2O)_3(HF)^5H$	155.070	2323
225	$(H_2O)^8(HF)^4H$	225.117	300
413	$UO_3(H_2O)_7H$	413.117	2323
449	$UO_2F_2(HF)_7H$	449.088	Both
462	$UO_2F_2(HF)_5(H_2O)_3$	462.100	300
518	$UF_6(HF)_2(H_2O)_7$	518.127	300
518[a]	$\mathbf{UF_5OH{\cdot}(HF)_3{\cdot}(H_2O)_6}$	**518.217**	**300**
523	$UO_2F_2(HF)_8(H_2O)_3H$	523.126	2323
537	$UO_2F_2(HF)_6(H_2O)_6H$	537.146	Both
605	$UO_2F_2(HF)_4(H_2O)_{12}H$	605.196	Both
634	$(UO_2F_2)_2(H_2O)$	634.085	Both
657	$(UO_2F_2)_2(HF)_2H$	657.095	2323
663	U_2OF_9	663.082	300
677	$U_2O_3F_6(HF)(H_2O)H$	677.101	300
733	$U_2O_3F_6(HF)_2(H_2O)_3H$	733.128	300
740	$UO_2F_2(HF)_4(UF_6)$	740.103	2323
808	$U_2O_3F_6(HF)_4(H_2O)_5$	808.154	300
837	$(UF_6)_2(H_2O)_4(HF)_3H$	837.151	2323
896	$(UO_3)_3(HF)(H_2O)$	896.123	2323
917	$(UO_3)_3(HF)_2(H_2O)H$	917.137	Both
954	$(UO_3)_3(HF)_3(H_2O)_2$	954.146	2323
964	$(UO_2F_2)_3(HF)_2$	964.124	300
976	$(UO_3)(UO_2F_2)_2(HF)(H_2O)_3$	976.148	Both
989	$(UO_2F_2)_2UF_6H_2F$	989.130	300

[a] Indicates a possible alternative formula.

Based on our data, we believe that instead of 4 single molecules of HF, a cluster of four HFs is most likely released as a single unit, which was directly measured by the MBMS at mass 81. Again, the strong hydrogen bonding among the HF molecules stabilizes the $(HF)_4^-$ cluster, allowing it to attract an H^+ to form $(HF)_4H$, which was a plausible explanation for the enhanced signal intensity of mass 81. The second most prominent molecule was the peak at 79, which was assigned as a protonated three-HF cluster with a single H_2O. The elevated concentration of $(HF)_3(H_2O)H$ cluster species measured was related to the stability of four HF molecules identified in the peak of 81 *m*/*z*. The missing HF molecule was replaced with protonated water, which could maintain the structural integrity of the cluster $(HF)_3(H_2O)H$. The stabilization of these molecules should be further examined using modelling as well as other spectroscopic techniques.

Masses above 400 *m*/*z* were classified as monomeric (400–610 *m*/*z*), dimeric (630–850 *m*/*z*), and trimeric (900–1000) uranium compounds. Monomeric compounds include a mixture of UO_2F_2, UF_6, UO_3, HF, and H_2O clusters. The presence of UF_6 for some compounds [*e.g.*, $UF_6(HF)_2(H_2O)_7$] indicates that such compounds existed primarily during the early stage of forming intermediate species or the limited water concentration. This is consistent with the comparison of 1.3% and 10% Rh conditions, where $UF_6(HF)_2(H_2O)_7$ had a higher signal at lower water concentration. At 1.3% Rh, the calculated moisture volume concentration was 300 ppm at 1 atm and 20 °C, thus UF_6 is still in excess stoichiometrically compared to water according to the molar ratio, defined by omega (ω) = $[H_2O]/[UF_6]$,[7] which is 1.51 for this condition. The choice of this ω value constrains the experimental condition at the upper limit of the water-restricted regime, beyond which the reaction pathway would start to shift and lean toward the water-rich regime where our 10% Rh described below was. On the other hand, monomeric compounds with UO_3 [*e.g.*, $UO_3(H_2O)_7$] were the products of late-step hydrolysis or the presence of excess water in the reaction mixture. Hydrolysis of UF_6 was suggested to proceed stepwise, with a series of compounds between UF_6 and UO_3.[3] UO_3 compounds were inferred to be formed from subsequent hydrolysis of UO_2F_2, which reduced the fluorine-to-oxygen ratio (F/U) from two to zero. At 10% Rh, the calculated moisture volume was 2323 ppm, which was significantly enhanced compared to 200 ppm of UF_6. The determined ω for this case was 11.62, an order of magnitude higher than the 300 ppm H_2O condition (ω = 1.51). Thus, a different cluster population was produced as shown in Table 1.

Dimers and trimers showed a similar pattern with the monomer, where the UF_6 and UO_3 occurred mostly in clusters produced in relatively dry and wet conditions, respectively. The compounds $(UO_3)_3(HF)_3(H_2O)_2$ and $(UO_3)_3(HF)(H_2O)$ occurred dominantly in 2323 ppm H_2O conditions, consistent with the U–O–F hydrolysis series. Uranium compounds with UO_2F_2 in the dimer and trimers (*e.g.*, $(UO_2F_2)_2(H_2O)$ and $UO_2F_2(HF)_4(H_2O)_{12}$) as one of the clusters reported the same variability for 300 and 2323 ppm of H_2O conditions. Moreover, the uranium compound U_2OF_9 at mass 663 was proposed to be an oxygen-bridged diuranium intermediate.

Overall, the identification of the uranium compounds and the HF-H_2O clusters was consistent with the water conditions during the hydrolysis of UF_6 forming the UO_2F_2 and HF products. Another important implication here is the vast difference in the molecular formula identified experimentally compared with the species presented in two prior theoretical studies.[4,5] UOF_4 was not identified in all the measurement trials, regardless of the precursor concentration.

The theoretical studies also indicated the formation of several dimers such as $(UF_5OH)_2$, $(UF_5)_2O$, and $U_2O_2F_9H$, all of which are based on the generation of key intermediate UF_5OH in the initial step of the UF_6 hydrolysis. The formation of this cluster was unfavourable for one or two water reactions.[4,5] When in high humidity conditions, *e.g.*, a three-water reaction, the formation of the UF_5OH pathway becomes favourable.[14] However, the absence of such compounds in our mass spectrum in both water conditions, particularly in the 2323 ppm water concentration was likely to indicate that this intermediate species might have a lifetime too short to permit observation in our experimental conditions. In other words, this cluster species (UF_5OH, mass 350) might serve as the core of a cluster species that combined with other smaller clusters in collision to form a stable cluster of mass higher than 350, such as UF_5-$OH{\cdot}(HF)_3{\cdot}(H_2O)_6$ with a mass of 518, which was found prevalent at ω = 1.51 condition. This is a borderline reaction condition such as the 1 to 2 water reaction scenario discussed previously, which was unfavourable for the core cluster UF_5OH to survive by itself without coordination with other clusters. Thus, coupling with smaller clusters would enable this cluster species to survive in a water-lean condition. Still, mass 350 was not identified as a prevalent peak in all our experiments including that of ω = 11.62. This result is further indication that the UF_5OH cluster could be formed as the theory predicted in water-rich conditions but it could only survive as a complex cluster.

We think the cluster of mass 663 should be written as U_2OF_9 because the $[U_2OF_9]^+$ ion could be the evidence for the presence of the previously predicted[4,5,14] oxygen bridged $(UF_5)_2O$ dimer as the $[U_2OF_9]^+$ ion could be a $(UF_5)_2O$ dimer that lost an F^-.

Atomic ratios of the determined uranium compounds impart relevant insights regarding the products of the UF_6 hydrolysis. The hydrogen-to-uranium ratio (H/U) is an indication of the extent of integration of H_2O molecules to UF_6 during hydrolysis. Also, fluorine to uranium ratio (F/U) showcases the stepwise hydrolysis of UF_6, with compounds at the latter stage reporting a higher F/U ratio. Fig. 3 shows the 3D map of the H/U, F/U, and masses of the products of the hydrolysis for both 300 (top) and 2323 (bottom) ppm water.

The size of the circles indicates the% difference of signals observed during hydrolysis and baseline measurements. The

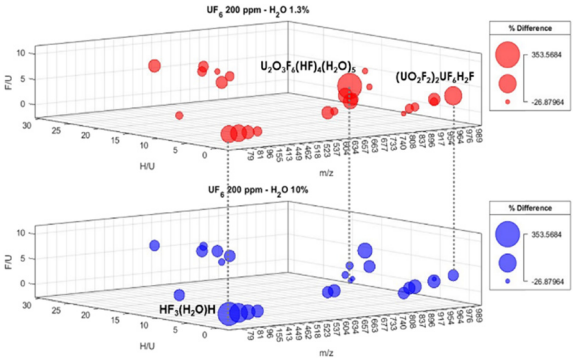

Fig. 3 3D map of the F/U, H/U, % difference, and masses of the identified non-uranium, monomeric, dimeric, and trimeric species.

3D space clearly distinguished the monomeric, dimeric, and trimeric uranium compounds. For instance, monomeric compounds are marked with high H/U, intermediate F/U values with a mass range between 400 to 600 *m*/*z*. Dimeric and trimeric compounds, on the other hand, had low H/U ratios. Also evident in the 3D plot is the difference in the concentration of the key species that are primarily observed in certain water conditions. These include $U_2O_3F_6(HF)_4(H_2O)_5$ and $(UO_2F_2)UF_6H_2F$, which were produced at low water conditions. HF trimer with H_2O monomer appreciably increased in high water conditions, which shows the potential of such compound to be a tracer of high humidity conditions during UF_6 hydrolysis reactions.

3.2. UF_6 ramping with fixed water concentration

To further understand the variability of the reaction intermediate species and end products, the concentration of UF_6 was ramped from 50 ppm to 231 ppm while holding the concentration of water constant (300 ppm H_2O). This was the range of ω of 6 to 1.3 corresponding to 50 ppm and 231 ppm UF_6 concentration, respectively. Shifting from H_2O-rich to UF_6 dominant conditions may provide insight into the formation schemes of the intermediates and products of the UF_6 hydrolysis from a view different from varying H_2O concentrations.[7] Fig. 4 shows the profile of masses 79, 81, and 96, which were still observed as the prevalent non-uranium compounds. The signal intensity corresponds to 4.3–8.7, 11.4–33.8, and 4.3 to 6.5 ppm concentration range for 79, 81, and 96 masses using the mass 333 calibration factors. The slopes of the best-fit lines are 0.624, 3.9174, and 0.377, with a coefficient of determination (r^2) at least of 0.97. Across the three trials, the three masses showed a consistent increase with the increasing concentration of UF_6. This confirmed that such fluorinated-water clusters ($(HF)_3(H_2O)H$, $(HF)_4H$, and $(H_2O)_2(HF)_3$) are dependent on the mixing ratio of UF_6 during the hydrolysis process, which was defined by the ω value that further supports the results presented.[7]

Interestingly, not all masses follow an increasing linear trend, which implies a different reaction formation pathway under different precursor conditions. Fig. 4 shows the average profile across three trials of the peaks listed in Table 1. The blue lines indicate an increasing signal while the red lines signify the reverse trend. Among the 949 peaks measured from mass 51 to 999, 527 ions had a positive slope while the remaining 422 ions did otherwise.

This constitutes a 55 to 45 ratio of ions with increasing and decreasing trends. In Fig. 4, one of the notable ions was mass 917, which was identified as $(UO_3)_3(HF)_2(H_2O)H$. It showed a decreasing trend, which indicates that its presence is depleted as the condition approaches UF_6-rich or water-lean conditions. The molecular identification of the peak was consistent with its trend, given the UO_3 trimer core of the cluster. As indicated before, intermediate products containing UO_3 were generated from the UF_6 hydrolysis upon subsequent exposure to UO_2F_2 at higher moisture conditions.

4. Summary and conclusion

The products of the UF_6 hydrolysis, an important nuclear material for energy production, were probed using the molecular beam mass spectrometer. This study utilized different H_2O and UF_6 conditions to determine intermediates and products of the hydrolysis, spanning from mass 50 to 1000 Daltons. Analysis of the mass spectra identified 26 major ions that had consistent appearances across three trial measurements. Each ion had different trends under different precursor concentrations. The major ions were clustered as non-uranium compounds, monomeric, dimeric, and trimeric compounds with varying numbers of H_2O and HF units. Non-uranium compounds were characterized by clusters of HF and H_2O units, whose profiles follow closely the variability of the UF_6 precursor. In the 3-D space continuum of F/U and H/U ratios, the non-uranium compounds showed low ratios for both atomic ratios. Monomeric compounds, found at the mass range between 400 to 600 *m*/*z*, exhibited high hydrogen-to-uranium ratios. In some ions, these monomeric species contain more than eight HF and H_2O units in their structure, resulting in high H/U ratios. Dimeric and trimeric species, occurring above mass 600, showed similar profiles with low H/U and intermediate F/U values.

Molecular identification of the major ions showed UF_6 and UO_3 as one of the core units of some of the intermediate and products of the hydrolysis. UF_6-related compounds (*e.g.*, $UF_6(HF)_2(H_2O)_7$) were prominent during the water-deprived conditions, consistent with the hydrolysis chain reactions of UF_6. On the other hand, compounds with UO_3 as one of their core compounds (*e.g.*, $UO_3(H_2O)_7$ and $(UO_3)_3(HF)_3(H_2O)_2$) were showing up in high moisture conditions (Rh = 10%, 2323 ppm H_2O) experiments. Expanding the molecular identification beyond the set parameters (*i.e.*, U, F, H and O atom numbers) might also reveal other uranium compounds with UF_6 and UO_3 in their chemical structures.

Furthermore, ramping UF_6 at constant H_2O conditions revealed different trends of the ions. Non-uranium compounds such as mass peaks of 79, 81, and 96 followed

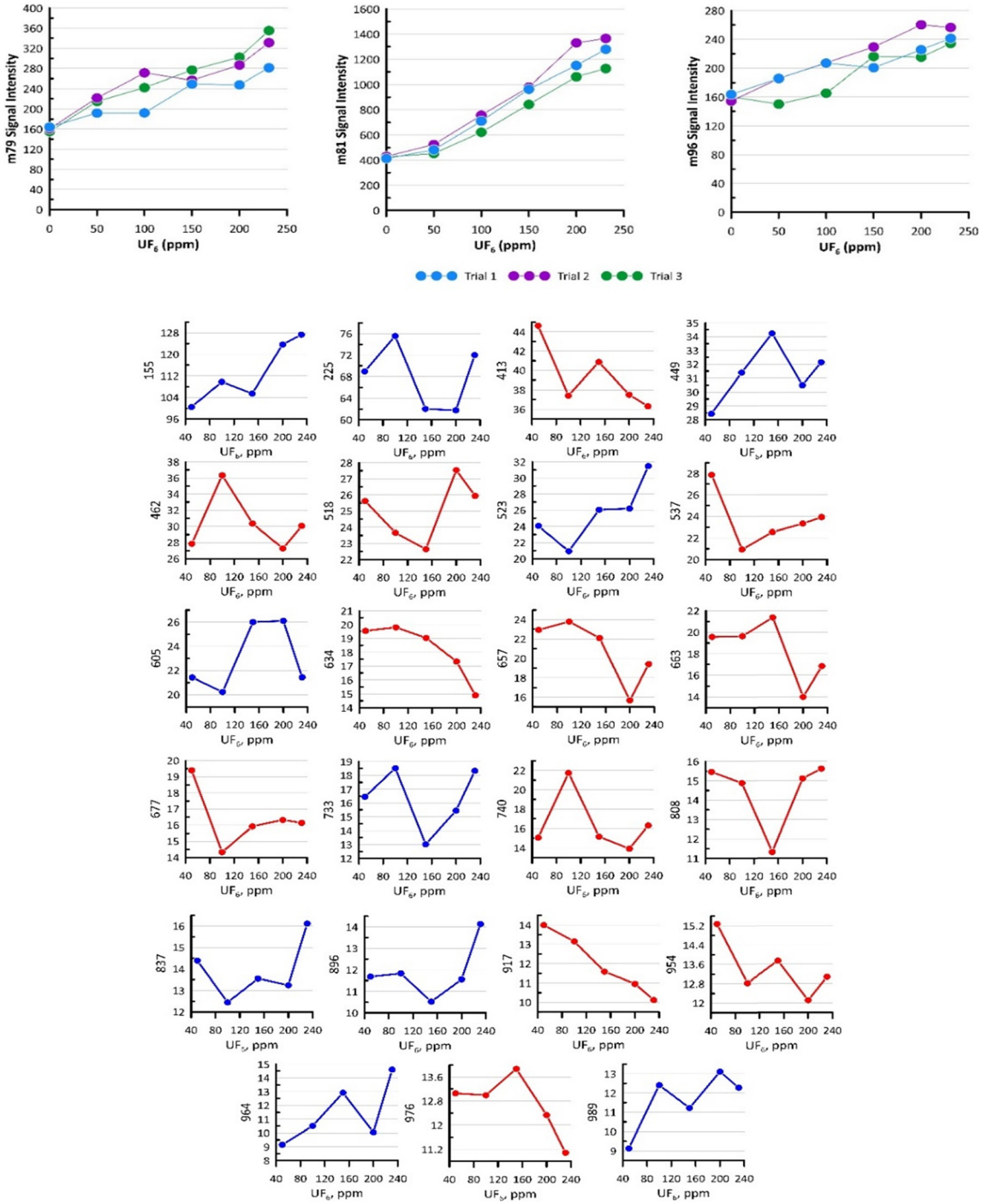

Fig. 4 (Top) Signal intensity of the non-uranium species $(HF)_3(H_2O)H$ (m79), $(HF)_4H$ (m81), and $(H_2O)_2(HF)_3$ (m96) across different trials. The signal intensity corresponds to 4.3–8.7, 11.4–33.8, and 4.3 to 6.5 ppm concentration range for 79, 81, and 96 masses using mass 333 calibration factors. (Bottom) Average intensities of masses presented in Table 1 as the UF_6 concentration increased. The blue lines indicate an increasing trend and the red indicate a decreasing trend.

the concentration of the introduced UF_6. On the other hand, several ions showed a reverse trend, in which a higher signal was observed during water-rich conditions. Some of the peaks such as the ion a 917, which was identified as $(UO_3)_3(HF)_2(H_2O)H$, had a consistent profile in which UO_3-related compounds are expected to occur in such conditions.

The vast amount of the data generated from the MBMS in different UF_6, and H_2O conditions merits a multivariate approach that will deliver in-depth information regarding the reaction formation of UF_6 hydrolysis. Cluster evaluation such as Calinski-Harabasz criterion clustering and factorization such as non-negative matrix factorization should be explored

to fully maximize the data generated from the MBMS, which would be highly relevant to the investigation of nuclear chemistry of uranium species in the atmosphere and surrounding environment.

Author contributions

Christian Mark Salvador: conceptualization, methodology, investigation, writing – original draft, formal analysis. Jason Richards: methodology, investigation, writing – original draft, formal analysis. Shannon Mahurin: methodology, conceptualization. Meng-Dawn Cheng: conceptualization, formal analysis, writing, resources, supervision, communication, funding acquisition, and correspondence should be addressed. Joshua Hubbard: computer simulation, writing.

Conflicts of interest

The authors do not have conflicts to declare.

Acknowledgements

This research was supported by the National Nuclear Security Administration of the Department of Energy. Oak Ridge National Laboratory is managed by UT-Battelle, LLC for the U. S. Department of Energy under contract DE-AC05-00OR22725. Sandia National Laboratories is a multi-mission laboratory managed and operated by National Technology & Engineering Solutions of Sandia, LLC, a wholly-owned subsidiary of Honeywell International Inc., for the U.S. Department of Energy's National Nuclear Security Administration under contract DE-NA0003525. This paper describes objective technical results and analysis. The research was funded by the National Nuclear Security Administration. Any subjective views or opinions that might be expressed in the paper do not necessarily represent the views of the U.S. Department of Energy or the United States Government. The United States Government retains and the publisher, by accepting the article for publication, acknowledges that the United States Government retains a non-exclusive, paid-up, irrevocable, world-wide license to publish or reproduce the published form of this manuscript or allow others to do so, for United States Government purposes. The Department of Energy will provide public access to these results of federally sponsored research in accordance with the DOE Public Access Plan (**https://energy.gov/downloads/doe-public-access-plan**).

References

1 R. Hou, T. Mahmud, N. Prodromidis, K. J. Roberts, R. A. Williams, D. T. Goddard and T. Semeraz, *Ind. Eng. Chem. Res.*, 2007, **46**, 2020–2033.
2 M. C. Lind, S. L. Garrison and J. M. Becnel, *J. Phys. Chem. A*, 2010, **114**, 4641–4646.
3 M. G. Otey and R. A. LeDoux, *J. Inorg. Nucl. Chem.*, 1967, **29**, 2249–2256.
4 S.-W. Hu, X.-Y. Wang, T.-W. Chu and X.-Q. Liu, *J. Phys. Chem. A*, 2008, **112**, 8877–8883.
5 S.-W. Hu, X.-Y. Wang, T.-W. Chu and X.-Q. Liu, *J. Phys. Chem. A*, 2009, **113**, 9243–9248.
6 J. M. Richards, L. R. Martin, G. A. Fugate and M.-D. Cheng, *RSC Adv.*, 2020, **10**, 34729–34731.
7 M.-D. Cheng, J. M. Richards, M. A. Omana, J. A. Hubbard and G. A. Fugate, *React. Chem. Eng.*, 2020, **5**, 1708–1718.
8 R. Horn, K. Ihmann, J. Ihmann, F. C. Jentoft, M. Geske, A. Taha, K. Pelzer and R. Schlögl, *Rev. Sci. Instrum.*, 2006, **77**(5), 054102.
9 A. Nag, A. Gerritsen, C. Doeppke and A. E. Harman-Ware, *Int. J. Mol. Sci.*, 2021, **22**, 4107.
10 R. Sykes, B. Kodrzycki, G. Tuskan, K. Foutz and M. Davis, *Wood Sci. Technol.*, 2008, **42**, 649–661.
11 A. E. Harman-Ware, D. Macaya-Sanz, C. R. Abeyratne, C. Doeppke, K. Haiby, G. A. Tuskan, B. Stanton, S. P. DiFazio and M. F. Davis, *Biotechnol. Biofuels*, 2021, **14**, 59.
12 L. Patiny and A. Borel, *J. Chem. Inf. Model.*, 2013, **53**, 1223–1228.
13 D. P. Armstrong, W. D. Bostick and W. H. Fletcher, *Appl. Spectrosc.*, 1991, **45**, 1008–1016.
14 S.-W. Hu, H. Lin, X.-Y. Wang and T.-W. Chu, *J. Mol. Struct.*, 2014, **1062**, 29–34.
15 O. P. Korobeinichev, S. B. Ilyin, V. V. Mokrushin and A. G. Shimakov, *Combust. Sci. Technol.*, 1996, **116–117**, 51–67.
16 K.-P. Hinz and B. Spengler, *J. Mass Spectrom.*, 2007, **42**, 843–860.
17 S. Kluge, H. Wiggers and C. Schulz, *Proc. Combust. Inst.*, 2017, **36**, 1037–1044.